Providing infrastructure for the Community Fault Model (CFM) to support SCEC science, community model development, and hazard assessment

Report for SCEC Award #19102
Submitted March 2020

Investigators: John H. Shaw and Andreas Plesch (Harvard), Scott T. Marshall (Appalachian State), and Phil Maechling (USC)

I. Project Overview ..... **i**
A. Abstract i
B. SCEC Annual Science Highlights i
C. Exemplary Figure i
D. SCEC Science Priorities ii
E. Intellectual Merit ii
F. Broader Impacts ii
G. Project Publications iii

II. Technical Report **1**
A. Summary 1
B. The New CFM Web Interface and Backend Database 1
C. New CFM Website Content 2
D. Updated Fault Representations for the 2019 M7.1 Ridgecrest Sequence 2
E. Regularized Fault Meshes 4
F. GFM Integration 4
G. References 5

I. Project Overview

A. Abstract

In the box below, describe the project objectives, methodology, and results obtained and their significance. If this work is a continuation of a multi-year SCEC-funded project, please include major research findings for all previous years in the abstract. (Maximum 250 words.)

The Community Fault Model (CFM) is one of SCEC's most established and widely used community models, with applications in many aspects of SCEC science, including crustal deformation modeling, wave propagation simulations, and probabilistic seismic hazards assessment (e.g., UCERF3). The CFM also directly contributes to other community modeling efforts, such as the Geological Framework (GFM), Community Rheologic (CRM), and Community Velocity (CVM-H) Models.

In collaboration with SCEC web developers, Meu-Hui Su, Edric Pauk, and Tran Huynh, we successfully developed and implemented a web-based viewer and search tool for the CFM (available at https://www.scec.org/research/cfm-viewer/). To facilitate increased modeling of the CFM within the greater SCEC community, the web-viewer also serves a new and improved set of preferred fault representations that utilize a nearly regularized mesh with 500, 1000, and 2000 meter element sizes. Based on user feedback, we have added content to the CFM homepage. This includes scripts for visualizing CFM faults, fault trace maps, a documentation that explains the GOCAD file format, and fault trace data. We have also developed a reproducible methodology for generating fault surfaces from data. We used this new methodology to update the CFM with new and improved fault representations including the source faults for the 2019 M7.1 Ridgecrest earthquake sequence and integrated the CFM with the GFM in a consistent manner. We anticipate that these new tools and model components will facilitate the next peer evaluation of the latest CFM version in future years and support UCERF and similar hazard assessment efforts.

B. SCEC Annual Science Highlights

Each year, the Science Planning Committee reviews and summarizes SCEC research accomplishments, and presents the results to the SCEC community and funding agencies. Rank (in order of preference) the sections in which you would like your project results to appear. Choose up to 3 working groups from below and re-order them according to your preference ranking.

CXM

C. Exemplary Figure

Select one figure from your project report that best exemplifies the significance of the results. The figure may be used in the SCEC Annual Science Highlights and chosen for the cover of the Annual Meeting Proceedings Volume. In the box below, enter the figure number from the project report, figure caption and figure credits.

Figure 1: web-based CFM query and download tool.

Figure 2: Map view of the final model of the 2019 Ridgecrest faults, including the Eastern and Southern Little Lake fault zones (colored surfaces). Focal Mechanisms and hypocenters are from Hauksson et al. (2012, 2020).

D. SCEC Science Priorities

In the box below, please list (in rank order) the SCEC priorities this project has achieved. See *https://www.scec.org/research/priorities* for list of SCEC research priorities. *For example: 6a, 6b, 6c*

P3a
P3b
P4a
P4c

E. Intellectual Merit

How does the project contribute to the overall intellectual merit of SCEC? *For example: How does the research contribute to advancing knowledge and understanding in the field and, more specifically, SCEC research objectives? To what extent has the activity developed creative and original concepts?*

This project contributes on an intellectual basis to SCEC in a variety of ways. The CFM, along with other SCEC Community Models, is used widely in many aspects of SCEC science, including crustal deformation modeling, wave propagation simulations, and probabilistic seismic hazards assessment (e.g., UCERF3). The CFM also directly contributes to other community modeling efforts, such as the Geological Framework Model (GFM), Community Rheologic (CRM), and Community Velocity (CVM-H) Models. This project is focused on delivering the model to practitioners, by developing and implementing a new web interface and associated database with the CFM object files and associated metadata. In addition, we developed a completely new methodology for developing tsurf representations that is reproducible and objective, thus supporting a wider range of CFM users.

F. Broader Impacts

How does the project contribute to the broader impacts of SCEC as a whole? *For example: How well has the activity promoted or supported teaching, training, and learning at your institution or across SCEC? If your project included a SCEC intern, what was his/her contribution? How has your project broadened the participation of underrepresented groups? To what extent has the project enhanced the infrastructure for research and education (e.g., facilities, instrumentation, networks, and partnerships)? What are some possible benefits of the activity to society?*

The project contributes supports one of SCEC's flagship Community Models (the CFM), and thus serves as a resource for the Center's primary mission of earthquake science and hazard assessment. By making the CFM more accessible to scientists, educators, and those professionally engaged in seismic hazard assessment and mitigation on an open website, these efforts help broaden the impact of SCEC and will lead to increased use of the CFM.

G. Project Publications

All publications and presentations of the work funded must be entered in the SCEC Publications database. Log in at *http://www.scec.org/user/login* and select the Publications button to enter the SCEC Publications System. Please either (a) update a publication record you previously submitted or (b) add new publication record(s) as needed. If you have any problems, please email *web@scec.org* for assistance.

II. Technical Report

A. Summary

The Community Fault Model (CFM; Plesch et al., 2007) is one of SCEC's most established and widely used community models, with applications in many aspects of SCEC science, including crustal deformation modeling, wave propagation simulations, and probabilistic seismic hazards assessment (e.g., UCERF3). The CFM also directly contributes to other community modeling efforts, such as the Geological Framework (GFM), Community Rheologic (CRM), and Community Velocity (CVM-H) Models.

2019 was a landmark year for the CFM. Our most significant accomplishment involves the release of the CFM web-based viewer and search tool (available at https://www.scec.org/research/cfm-viewer/, Fig. 1). In collaboration with SCEC web developers, Meu-Hui Su, Edric Pauk, and Tran Huynh, we successfully developed and implemented a web-based viewer and search tool for the CFM. To facilitate increased modeling of the CFM within the greater SCEC community, the web-viewer also serves a new and improved set of preferred fault representations that utilize a nearly regularized mesh with 500, 1000, and 2000 meter element sizes. We updated the CFM with new and improved fault representations including the source faults for the 2019 M7.1 Ridgecrest earthquake sequence and integrated the CFM with the Geological Framework Model (GFM) in a consistent manner. We have also added content to the CFM homepage based on user feedback. This includes scripts for visualizing CFM faults, fault trace maps, a document that explains the GOCAD file format, and fault trace data.

We anticipate that these new tools and model components will facilitate the next peer evaluation of the latest CFM version in future years and support UCERF or similar hazard assessment efforts.

B. The New CFM Web Interface and Backend Database

The CFM is an object-oriented, three-dimensional (3D) representation of active faults in southern California and adjacent offshore basins. As our knowledge of southern California's seismic sources improves, so does the complexity of the CFM. CFM currently contains 380 individually named fault representations and including alternative representations, incorporates more than 820 fault objects. Each of these objects exists as 3D triangulated representations (GOCAD t-surfs) of various fault surface components, as well as fault trace shapefiles, and associated metadata. In past years, the SCEC CFM was distributed as a collection of data files in a single archive, which required the user to uncompress the archive and search for desired objects manually. To make the CFM more accessible and useful to researchers, we have developed an interactive CFM website that provides a queryable and interactive map-based interface to the latest released version (CFM5.2) of preferred CFM faults. The new web interface enables users to search, view, and download the CFM faults using several criteria including keywords, geographic extent (latitude and longitude ranges), and several other criteria. The current site also allows users to download CFM fault geometry files in several selected formats/resolutions.

With the previous release of CFM5.2, faults are now represented in a hierarchical structure including Fault Area, Fault Zone, Fault Section, Fault Name, Splay, and Alternative designations. These designations are identical to those used in the USGS Qfault database, which ensures that users can properly relate fault information between the CFM and Qfault database, such as geometry and slip rate, respectively. Currently, all these fault components and attributes are organized in a master spreadsheet, which is provided for download on the CFM website. The challenge when creating the web viewer is that, in order for the CFM web-viewer to function, this relational database must contain unique, well defined, and immutable relationships between rows in the spreadsheet, t-surf geometric fault representations (and associated file

names), and objects in the GIS-type shapefiles of fault traces. These requirements are strict and demand fully error free and complete data. Achieving this for CFM5.2 was a time-consuming process and involved thousands of minor, but nonetheless necessary changes. During the past year, we have written several scripts to quality check many CFM components, but additional quality checks will need to be added to our codes to ensure seamless compatibility with future releases.

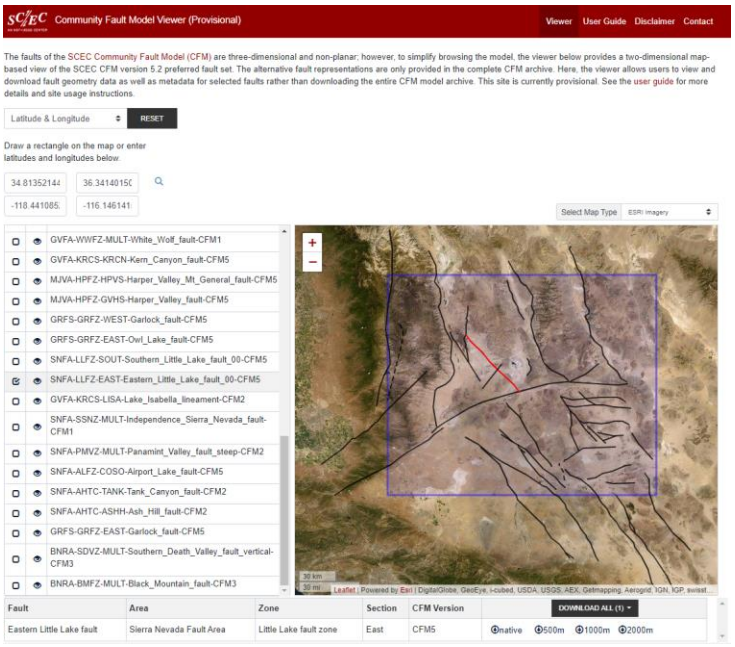

Figure 3: web-based CFM query and download tool.

The release of the CFM viewer website has resulted in several constructive user requests, many of which we propose to address with subsequent release of updated CFM and associated website enhancements. We continue to work with SCEC's science and software groups to develop the CFM viewer website using an iterative software development process in which SCEC scientists identify and prioritize desired capabilities. The SCEC software group then rapidly prototypes new features, and SCEC researchers review the site capabilities to ensure they provide value and ease of access to the science community. Several initial website reviews have already resulted in corrections to the CFM database as well as improvements to the viewer site. This software development process has served as a model as the CXM group works to create more web-based tools for the various CXM's.

C. New CFM Website Content

Along with the web interface, we also added new content to the CFM homepage including a significantly updated MATLAB-based CFM visualization tool (plotMesh.m). This tool is needed because, based on user feedback, many SCEC researchers do not have access to CAD software that can directly import and visualize GOCAD or any type 3D files. plotMesh.m provides a MATLAB-based algorithm for loading GOCAD surface data, visualizing CFM surfaces, and calculating directional statistics for a given CFM fault. We also created and posted:

1) A series of CFM fault trace maps with several different basemaps
2) Downloadable CFM5.2 trace data as both GIS shapefiles and GMT multi-segment files (ASCII)
3) A GOCAD file frequently asked questions document to help users better understand the content and structure of GOCAD t-surf files

D. Updated Fault Representations for the 2019 M7.1 Ridgecrest Sequence

We added new 3D source fault representations for the 2019 M6.4 and M7.1 Ridgecrest earthquake sequence to the CFM. These representations are based on relocated hypocenter catalogs expanded by template matching (Ross et al., 2019) and focal mechanisms for M4 and larger events (Hauksson et al.,

2020). Following the approach of Riesner et al. (2017), we generated reproducible 3D fault geometries by integrating hypocenter, nodal plane, and surface rupture trace constraints. We used the SW-NE striking nodal plane of the July 4th, 2019 M6.4 event to constrain the initial representation of the Southern Little Lake fault (SLLF) both in terms of location and orientation. The Eastern Little Lake fault (ELLF) was constrained by the July 5th, 2019 M7.1 hypocenter and nodal planes of M4 and larger aftershocks aligned with the main trend of the fault. The approach follows a defined workflow that assigns weights to a variety of geometric constraints. These main constraints have a high weight relative to that of individual hypocenters, ensuring that small aftershocks are applied as weaker constraints. The resulting fault planes can be considered averages of the hypocentral locations respecting nodal plane orientations. For the final representation we added detailed, field mapped rupture traces (Kendrick et al., 2019) as strong constraints. The resulting fault representations are generally smooth but non-planar and dip steeply. The two faults intersect each other at nearly right angles. The ELLF representation is truncated at the Airport Lake fault to the north and the Garlock fault to the South, consistent with the aftershock pattern. The terminations of the SLLF representation are controlled by aftershock distribution. These new 3D fault representations are available as triangulated surface representations for wider use. The CFM web interface currently has access to the two main fault surfaces with branches and cross-faults being in the process of being formally named, and added to the database.

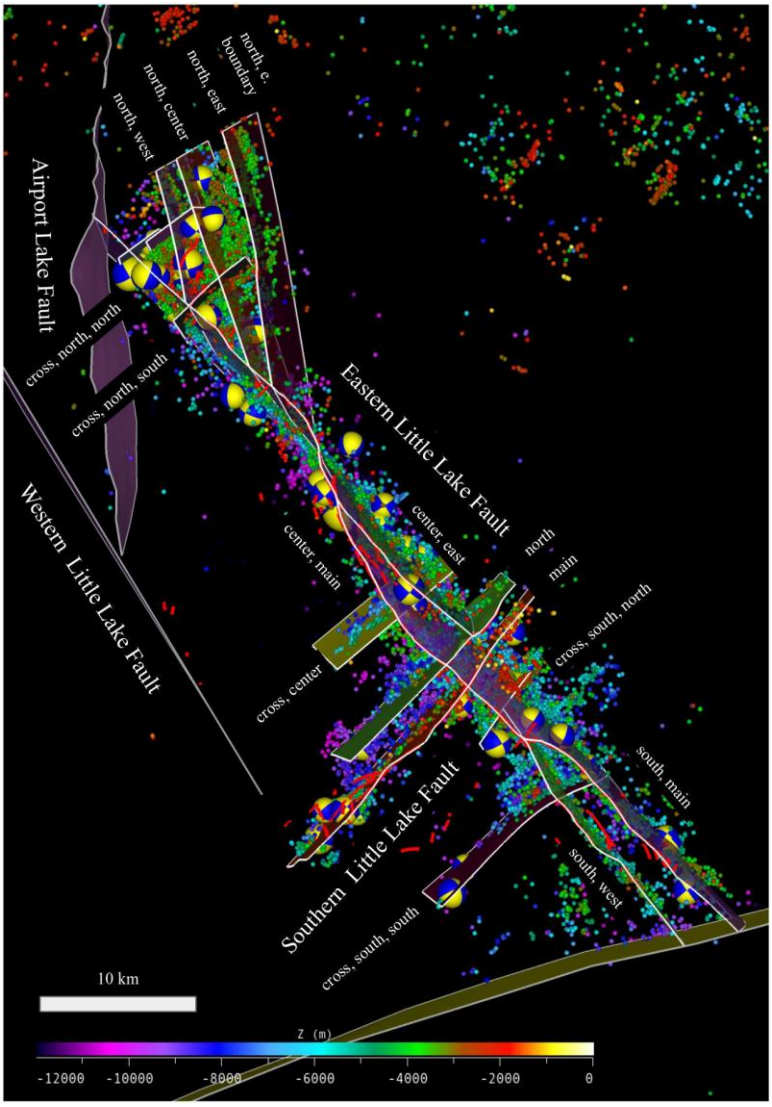

Figure 4: Map view of the final model of the 2019 Ridgecrest faults, including the Eastern and Southern Little Lake fault zones (colored surfaces). Focal Mechanisms and hypocenters are from Hauksson et al. (2012, 2020).

Our 3D source fault model of 2019 Ridgecrest earthquake sequence defines a complex system, consisting of two main ruptures representing the Southern and Eastern Little Lake faults and twelve additional fault splays (Fig. 2). The main southern Little Lake fault, associated with the 4 July 2019 M6.4 earthquake, extends for about 20 km in a northeast-southwest direction. The fault is steeply dipping (≥ 80°) but is non-planar, with components of northwest and southeast dip at various locations along strike. A second, northern fault splay extends for about 18 km along strike, and is defined by hypocenters, focal mechanisms, and surface ruptures along the eastern extent of the fault trace. Three additional northeast-southwest trending cross faults are modeled to the north and south of the Southern Little Lake fault.

The source fault representation for the 5 July M7.1 earthquake consists of an ≈ 60km long, northwest-southeast striking plane that we define as the Eastern Little Lake fault. The fault surface is illuminated by seismicity along most of its extent, while ground surface ruptures are generally limited to the central (≈ 40 km long) portion of the rupture. The fault dips steeply (≥ 55°) to the northeast in the center and along the southern extent of the rupture, and steepens to near vertical along the northern extent of the rupture. The fault becomes near vertical at depth along the entire extent of the rupture. There are two distinct sub-parallel splays to the south of the M7.1 mainshock epicentral zone. The M7.1 mainshock is associated with the western (main) fault splay. However, many of the larger foreshocks and aftershocks are associated with the eastern of these two fault splays. This eastern splay merges with the western splay to the north, but to the south appears to truncate into the northern splay of the Southern Little Lake fault. In contrast, the western segment of the Eastern Little Lake fault passes across the Southern Little Lake faults. About 18km south of the M7.1 mainshock, the fault has a second, sub-parallel (western) splay illuminated by seismicity and ground surface ruptures. These two splays extend south for about 18 km and truncate into the Garlock fault. To the north of the mainshock, the seismicity becomes more broadly distributed and small surface ruptures define both northwest-southeast and northeast-southwest trending elements. Our analysis defines that the northwest-southeast trending elements are consistent with a series of long (>8km) continuous fault segments. Specifically, our analysis of the hypocentral locations defines four fault segments that extend northward from the main trace of the Eastern Little Lake fault (Figure 2). These faults likely represent only the largest of a series of splays that define distributed deformation along the north extent of the rupture. The Eastern Little Lake fault terminates to the north into the Airport Lake fault. However, the northern splay faults are limited by the northern extent of the seismicity, and thus terminate to the south and east of the Airport Lake fault.

E. Regularized Fault Meshes

The triangulated meshes which natively come out of 3D characterization and construction of the CFM fault representations reflect the availability and distribution of underlying data sets. Their design goal is to define a surface with a sparse set of triangular elements and to avoid introducing elements for reasons other than data compliance such as mesh quality. On the other hand, many numerical applications require meshes which consist of similarly sized and shaped elements for computational accuracy. Therefore, we regenerated all faults in the CFM 5.2 version of the model, with 500m, 1000m, and 2000m average triangle size meshes. This remeshing task is not trivial since geometry and boundaries need to be preserved. For practical purposes, we relied on a commercial tool, the Finite Elements Mesh generator available in Emerson/Paradigm SKUA-GOCAD which is based on Lepage (2003). The process could be largely automated except for a number of native fault meshes that had completely degenerate triangles and needed to be manually reconstructed. All faults in the Preferred CFM5.2 now have regularized meshes available for download via the new CFM web interface.

F. GFM Integration

We integrated the CFM into a volumetric version of the SCEC Geologic Framework Model (GFM) which attempts to be compatible with other SCEC Community Models (CXMs) and which can be queried at any 3D location. The model is based on an initial definition of 23 lithotectonic units separated by major faults or contrasts in basement lithology and tectonic affinity. The base of model is located at 100 km depth. In order to achieve maximum compatibility with the CFM, we first identified all CFM fault representations which define block boundaries (Fig. 3). Then individual block boundaries were extracted at the surface level as map coverages. From those, first 3D template surfaces were constructed along the average dips of all CFM faults involved in a given boundary, down to the Moho level. Finally, these template surfaces were

smoothly fit to the detailed CFM fault representations. This procedure was first applied to the three boundaries which were recognized to have more complex, dipping attitudes: the northern and southern boundary of the Western Transverse Ranges, and the southern boundary of the San Gabriel block. Other boundaries are modeled currently with a vertical orientation. All boundaries are available as separate model components. From these bounding surfaces, a gridded volume was subdivided into regions. SCEC CME developed a prototype query interface which can be used to interrogate the model at any point and depth.

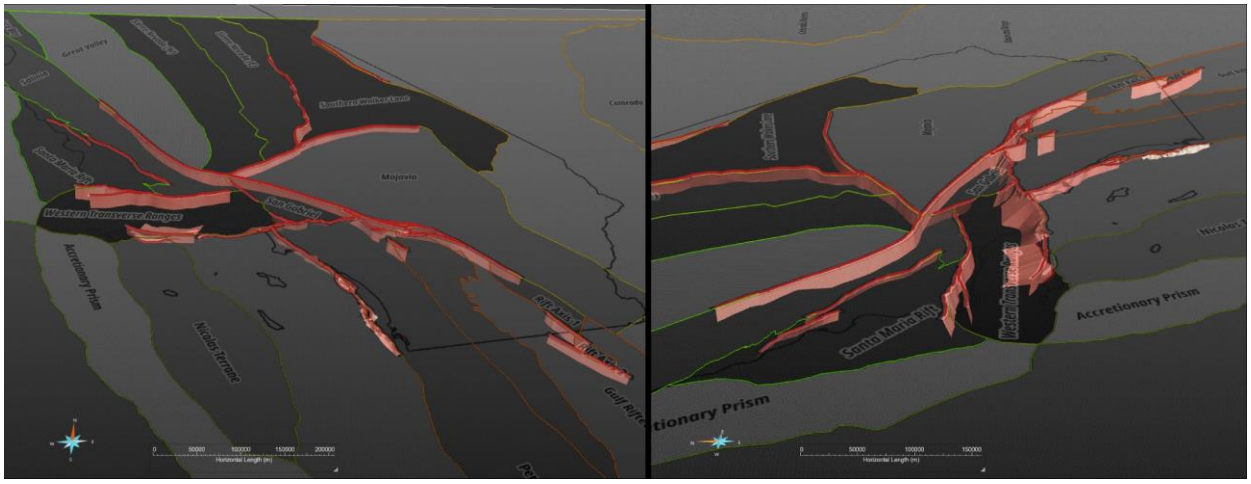

Figure 5: Perspectives views of CFM faults red surfaces) that represent boundaries between lithotectonic blocks (gray regions) in the GFM.

G. References

Hauksson, E., W. Yang, and P. M. Shearer, (2012), Waveform relocated earthquake catalog for southern california (1981 to June 2011), Bull. Seismol. Soc. Am., 102(5), 2239–2244.

Hauksson, E., C. Yoon, E. Yu, J. R. Andrews, M. Alvarez, R. Bhadha, and V. Thomas (2020). Caltech/USGS Southern California Seismic Network (SCSN) and Southern California Earthquake Data Center (SCEDC): Data Availability for the 2019 Ridgecrest Sequence, Seismol. Res. Lett., XX, 1–10, doi: 10.1785/0220190290.

Kendrick, K. J., Akciz, S. O., Angster, S. J., Avouac, J., Bachhuber, J. L., Bennett, S. E., Blake, K., Bork, S., Brooks, B. A., Burgess, P., Chupik, C., Dawson, T., DeFrisco, M. J., Delano, J., DeLong, S., Dolan, J. F., DuRoss, C. B., Ericksen, T., Frost, E., Gold, R. D., Graehl, N. A., Haddon, E. K., Hatem, A. E., Hernandez, J. L., Hitchcock, C., Hudnut, K. W., Koehler, R. D., Kozaci, O., Ladinsky, T., Madugo, C. M., Mareschal, M., McPhillips, D., Milliner, C., Morelan, A. E., Nevitt, J., Olson, B., Padilla, S. E., Patton, J. R., Philibosian, B., Pickering, A., Pierce, I., Ponti, D. J., Pridmore, C., Rosa, C., Roth, N., Scharer, K. M., Seitz, G. G., Spangler, E., Swanson, B. J., Thomas, K., Thompson Jobe, J., Treiman, J. A., Williams, A. M., & Oskin, M. E., (2019). Geologic observations of surface fault rupture associated with the Ridgecrest M6.4 and M7.1 earthquake sequence by the Ridgecrest Rupture Mapping Group, Poster Presentation at 2019 SCEC Annual Meeting, Palm Springs, CA.

Lepage. F. (2003), Generation de maillages tridimensionels pour la simulation des phenoenes physiques en geosciences. PhD thesis, Institut National Polytechnique de Lorraine, Nancy, France, 224 pp.

Lin, G., P. M. Shearer, and E. Hauksson, 2007, Applying a three-dimensional velocity model, waveform crosscorrelation, and cluster analysis to locate southern California seismicity from 1981 to 2005, J. Geophys. Res., v.112, n.B12, 14 pp, B12309, doi:10.1029/2007JB004986.

Plesch, A., J. H. Shaw, C. Benson, W. A. Bryant, S. Carena, M. Cooke, J. Dolan, G. Fuis, E. Gath, L. Grant, E. Hauksson, T. Jordan, M. Kamerling, M. Legg, S. Lindvall, H. Magistrale, C. Nicholson, N. Niemi, M. Oskin, S.

Perry, G. Planansky, T. Rockwell, P. Shearer, C. Sorlien, M. P. Süss, J. Suppe, J. Treiman, and R. Yeats, (2007), Community Fault Model (CFM) for Southern California, Bulletin of the Seismological Society of America, Vol. 97, No. 6, doi: 10.1785/012005021

Riesner, M., Durand-Riard, P., Hubbard, J., Plesch, A., and Shaw, J. H., (2017). Building Objective 3D Fault Representations in Active Tectonic Settings, SRL, 88. 10.1785/0220160192.

Ross, Z. E., Trugman, D. T., Hauksson, E., and Shearer, P. M., (2019). Searching for hidden earthquakes in Southern California, Science, 364/ 6442, 767-771.

Yang, W., E. Hauksson, and P.M. Shearer, P. M., (2012), Computing a large refined catalog of focal mechanisms for southern California (1981–2010): Temporal stability of the style of faulting. BSSA, 102(3), 1179-1194.